7th Heidelberg International Symposium on
High-Energy Gamma-Ray Astronomy (Gamma 2022)
Thursday, 7 July 2022 16:00 (15 minutes)

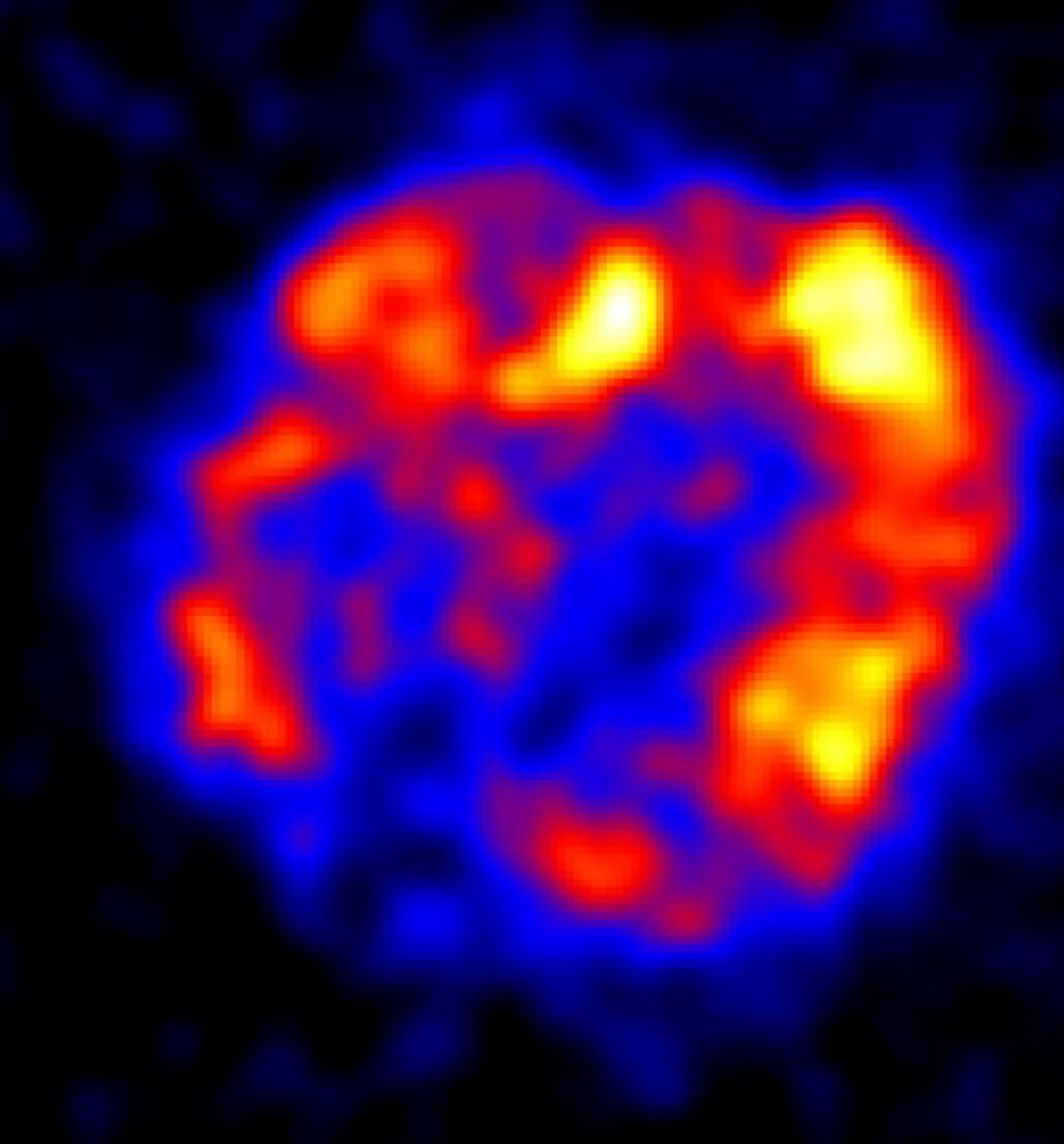

ALMA CO Observations in the Northwestern Shell of the Gamma-Ray SNR RX J1713.7-3946

Hidetoshi Sano (Gifu Univ.)

Co-authors: T. Inoue, K. Tokuda, T. Tanaka, R. Yamazaki, S. Inutsuka, F. Aharonian, G. Rowell, M. D. Filipovic, Y. Yamane, S. Yoshiike, N. Maxted, H. Uchida, T. Hayakawa, K. Tachihara, Y. Uchiyama, & Y. Fukui

web URL

Sano, Inoue, Tokuda et al. 2020c, ApJ Letters, 904, 24

ALMA CO Observations of the Gamma-Ray Supernova Remnant RX J1713.7-3946:
Discovery of Shocked Molecular Cloudlets and Filaments at 0.01 pc scales

H.E.S.S. TeV gamma-rays (H.E.S.S. Col. 2018)

SNR RX J1713.7−3946

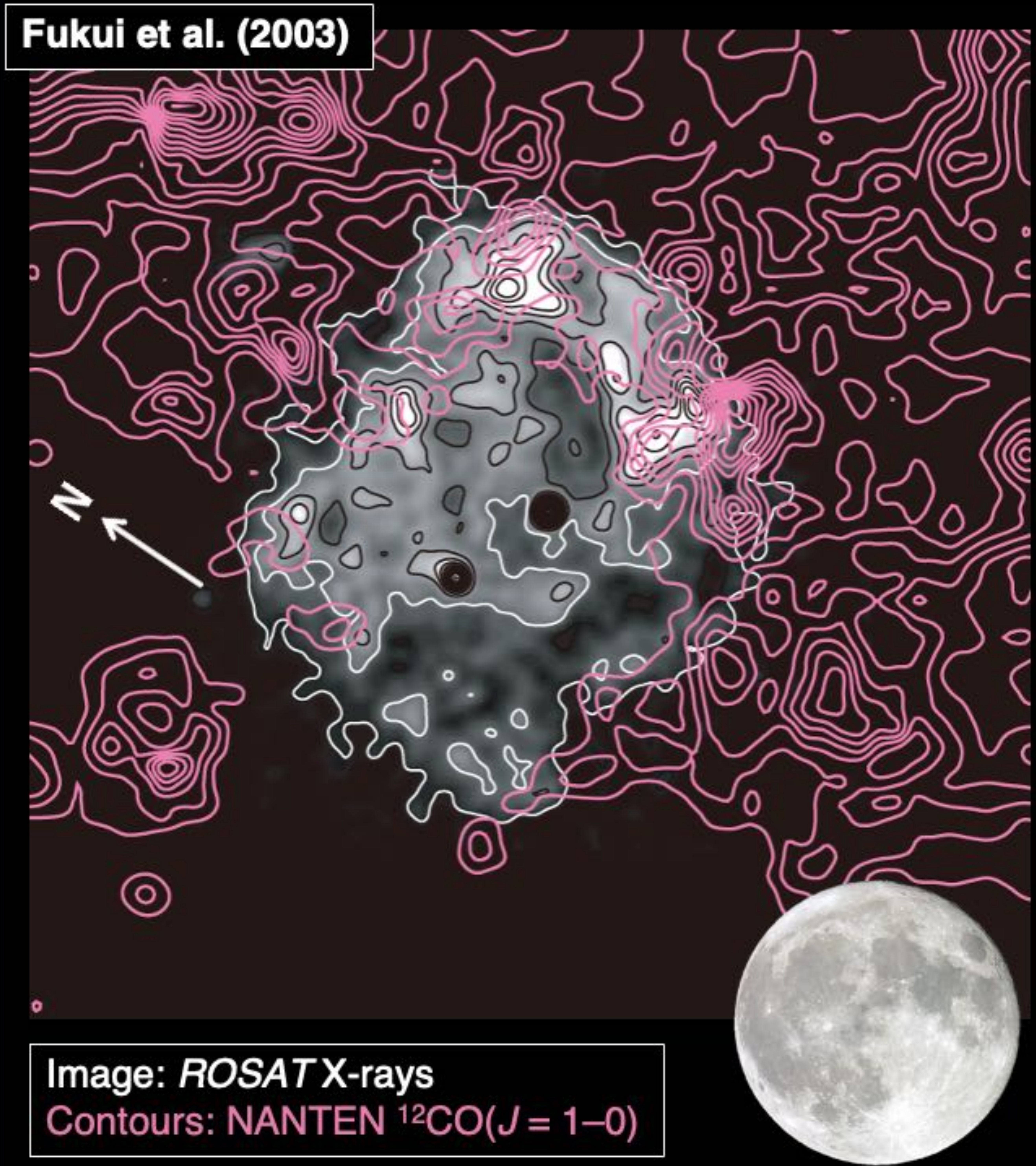

Fukui et al. (2003)

Image: *ROSAT* X-rays
Contours: NANTEN ^{12}CO(J = 1–0)

RX J1713.7–3946 (G347.3–0.5)

- Shell-type SNR discovered by *ROSAT*
  (Pfeffermann & Aschenbach 1996)
- Distance / Diameters : ~1 kpc / ~18 pc (~1°)
  (e.g., Fukui et al. 2003; Cassam-Chenaï et al. 2004; Leike et al. 2021)
- Age : ~1600 yr (SN 393)
  (Wang et al. 1997; Fukui et al. 2003; Tsuji & Uchiyama 2016)
- **Associated with molecular/atomic clouds**
  ➡ shock-cloud interaction with *B* amplification
  (e.g., Fukui et al. 2003, 2012, 2021; Moriguchi et al. 2005; Inoue et al. 2009, 2012; Sano et al. 2010, 2013, 2015, 2020; Maxted et al. 2012, 2013)
- TeV / GeV Gamma-rays
  ➡ Steep *νFν* spectrum + Hadron dominant
  (e.g., Muraishi et al. 2000; Aharonian et al. 2004, 2006, 2007; Zirakashvili & Aharonian 2010; Abdo et al. 2011; Inoue et al. 2012; Gabici & Aharonian 2014; H.E.S.S. Collaboration 2018; Celli et al. 2019; Inoue 2019; Fukui et al. 2021)
- **Synchrotron X-rays ➡ Time variation**
  (e.g., Koyama et al. 1997; Slane et al. 1999; Hiraga et al. 2005; Uchiyama et al. 2007; Takahashi et al. 2008; Tanaka et al. 2008, 2020; Acero et al. 2009; Sano et al. 2015; Okuno et al. 2018; Tsuji et al. 2019; Kuznetsova et al. 2019; Higurashi et al. 2020)

SNR RX J1713.7−3946: X-ray enhancement around the clouds


Fukui et al. (2003)

Sano et al. (2010, 2013)

Image: *ROSAT* X-rays
Contours: NANTEN ^{12}CO(J = 1–0)

Image: Suzaku X-rays (E: 5–10 keV)
Contours: NANTEN2 ^{12}CO(J = 2–1)

SNR RX J1713.7−3946: Spatial variation of photon indies

Fukui et al. (2003)

Image: *ROSAT* X-rays
Contours: NANTEN ^{12}CO(J = 1–0)

Sano et al. (2015)

Image: Synchrotron X-ray photon index
Contours: NANTEN2 ^{12}CO(J = 2–1)

SNR RX J1713.7−3946: Shock interactions with clumpy clouds

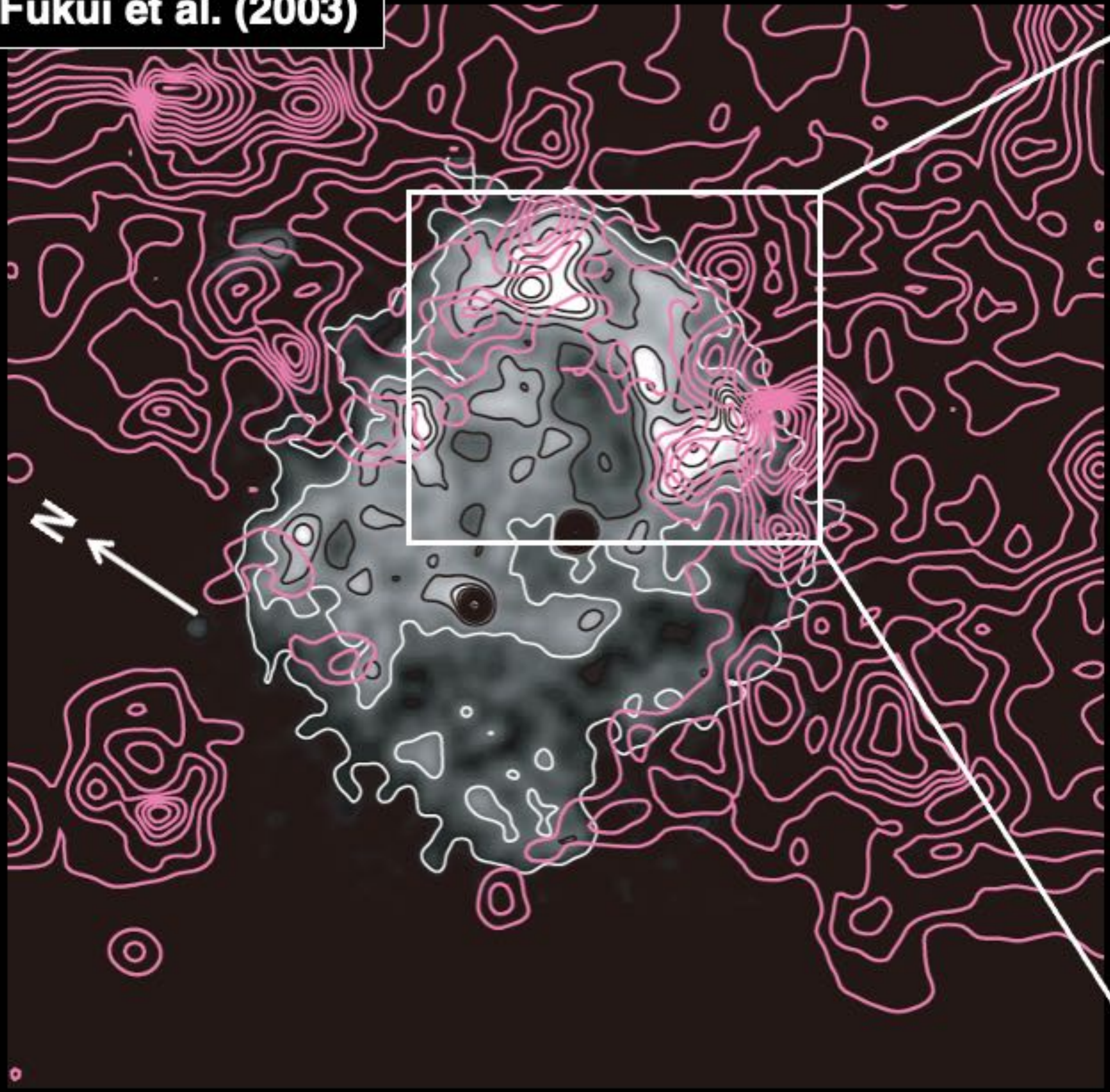

Fukui et al. (2003)

Image: *ROSAT* X-rays
Contours: NANTEN ^{12}CO(J = 1–0)

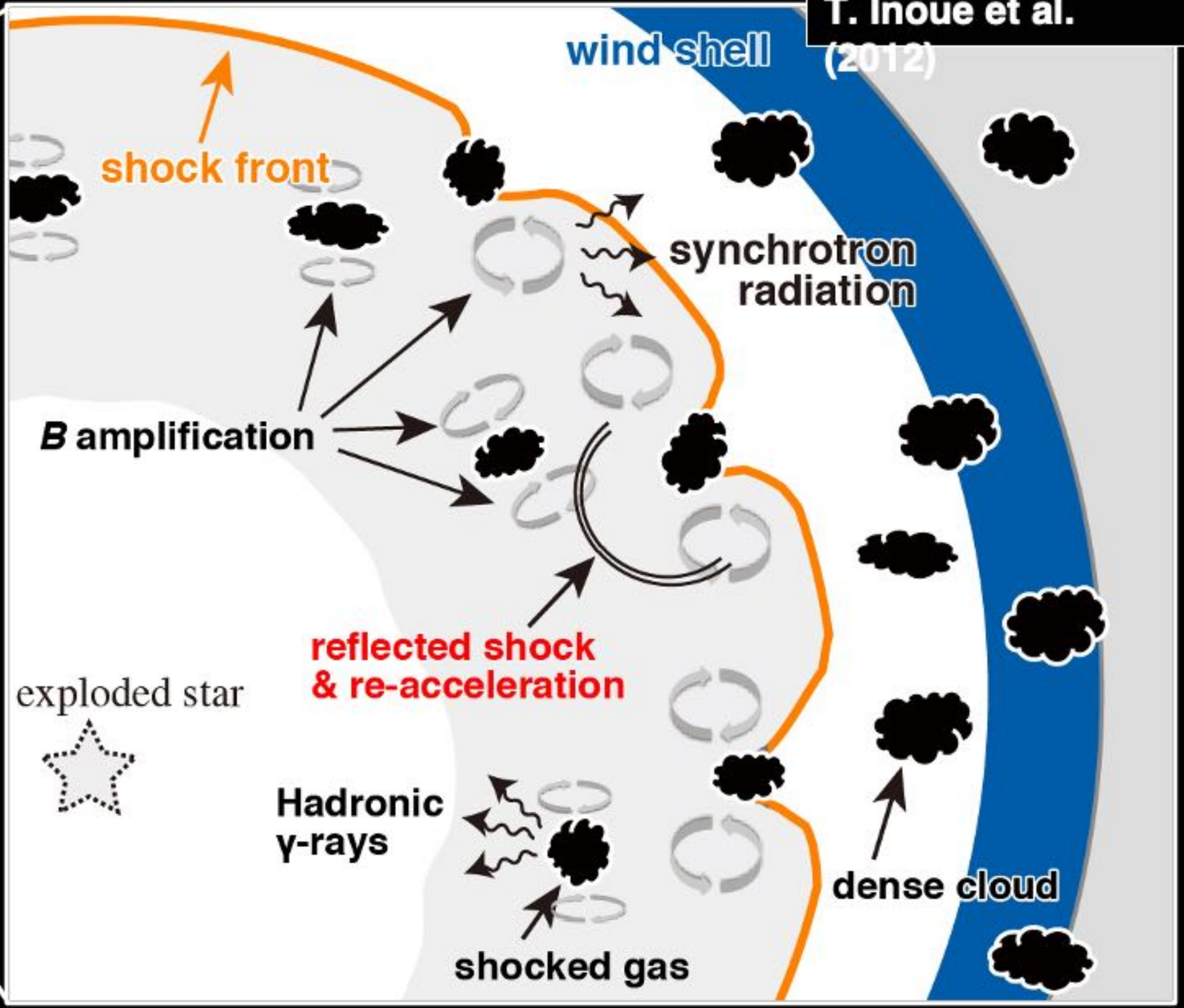

T. Inoue et al. (2012)

Schematic image of shock-cloud interaction
Cloud density: ~10^3 cm^{-3}, Intercloud density: ~0.01 cm^{-3}

SNR RX J1713.7−3946: Time variability of X-ray hot spots

Fukui et al. (2003)

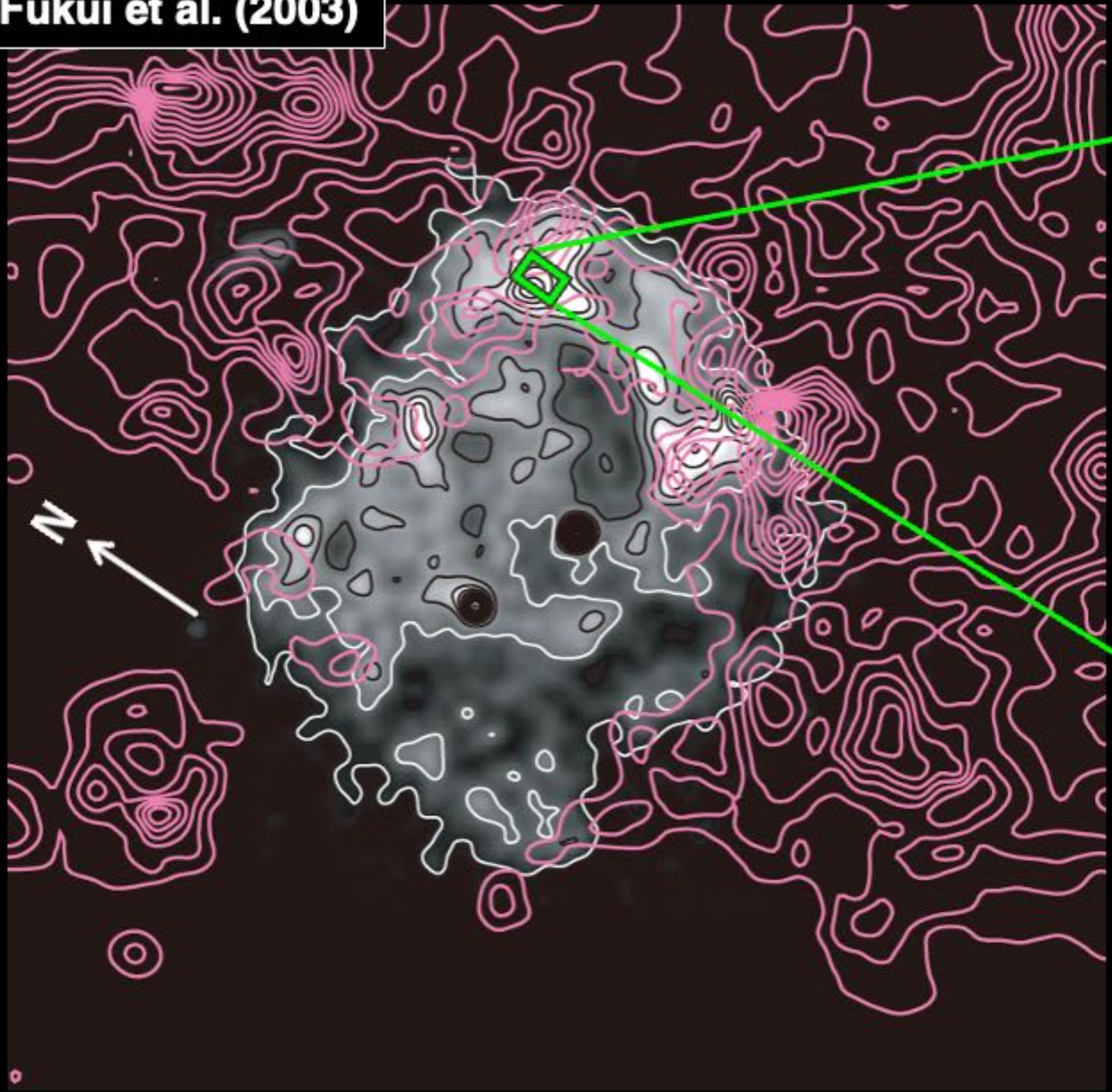

Image: *ROSAT* X-rays
Contours: NANTEN ^{12}CO(J = 1–0)

Uchiyama et al. (2007)

Images: Chandra X-rays

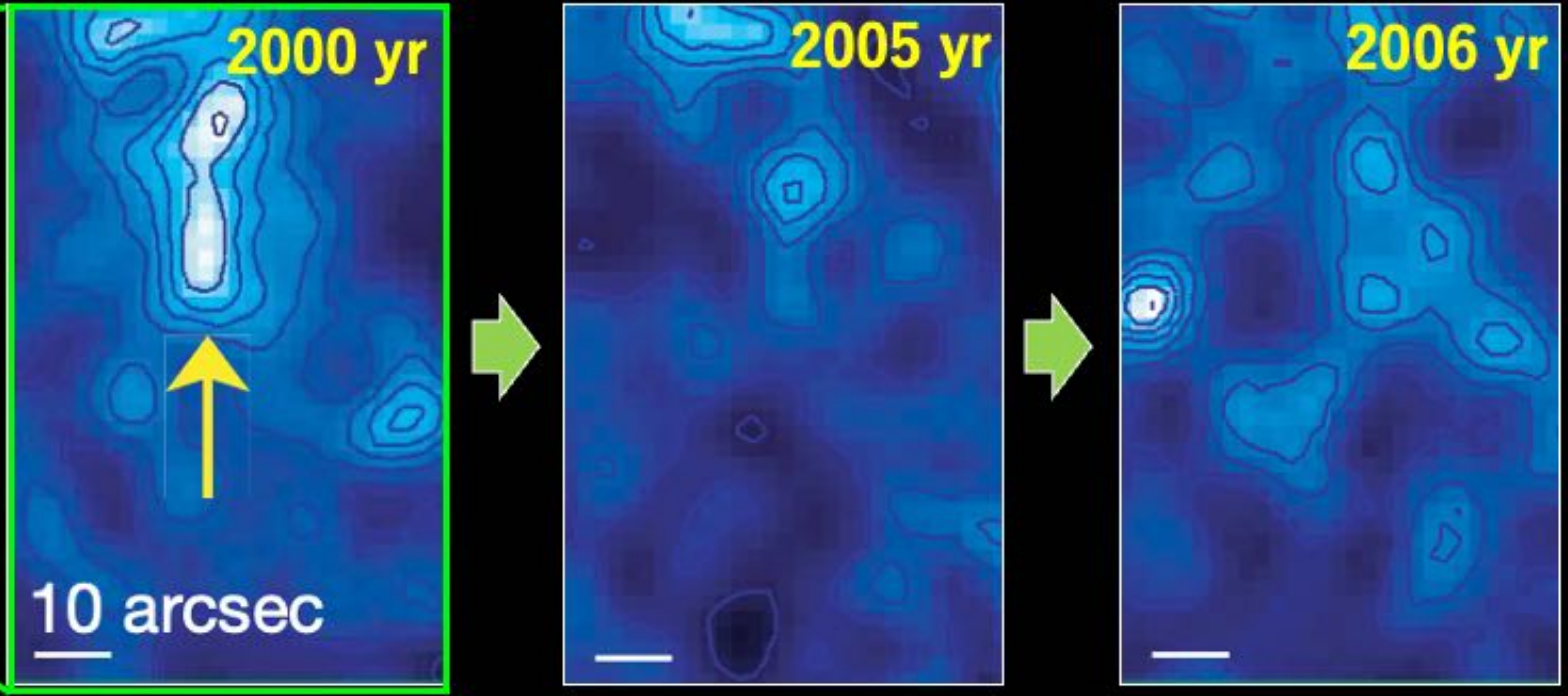

$$T_{\rm synch} \sim 1.5 \left(\frac{B}{1\ {\rm mG}}\right)^{-1.5} \left(\frac{\varepsilon}{1\ {\rm keV}}\right)^{-0.5} ({\rm yr})$$

$$T_{\rm acc} \sim 1\eta \left(\frac{B}{1\ {\rm mG}}\right)^{-1.5} \left(\frac{\varepsilon}{1\ {\rm keV}}\right)^{0.5} \left(\frac{V_{\rm s}}{3000\ {\rm km\ s^{-1}}}\right)^{-2} ({\rm yr})$$

X-ray hot spot shows *B* ~1 mG at 10 arcsec (~0.05 pc) scales

➡ Tiny clouds should be expected near the X-ray hot spots!?

ALMA CO observations toward the NW of RX J1713.7−3946

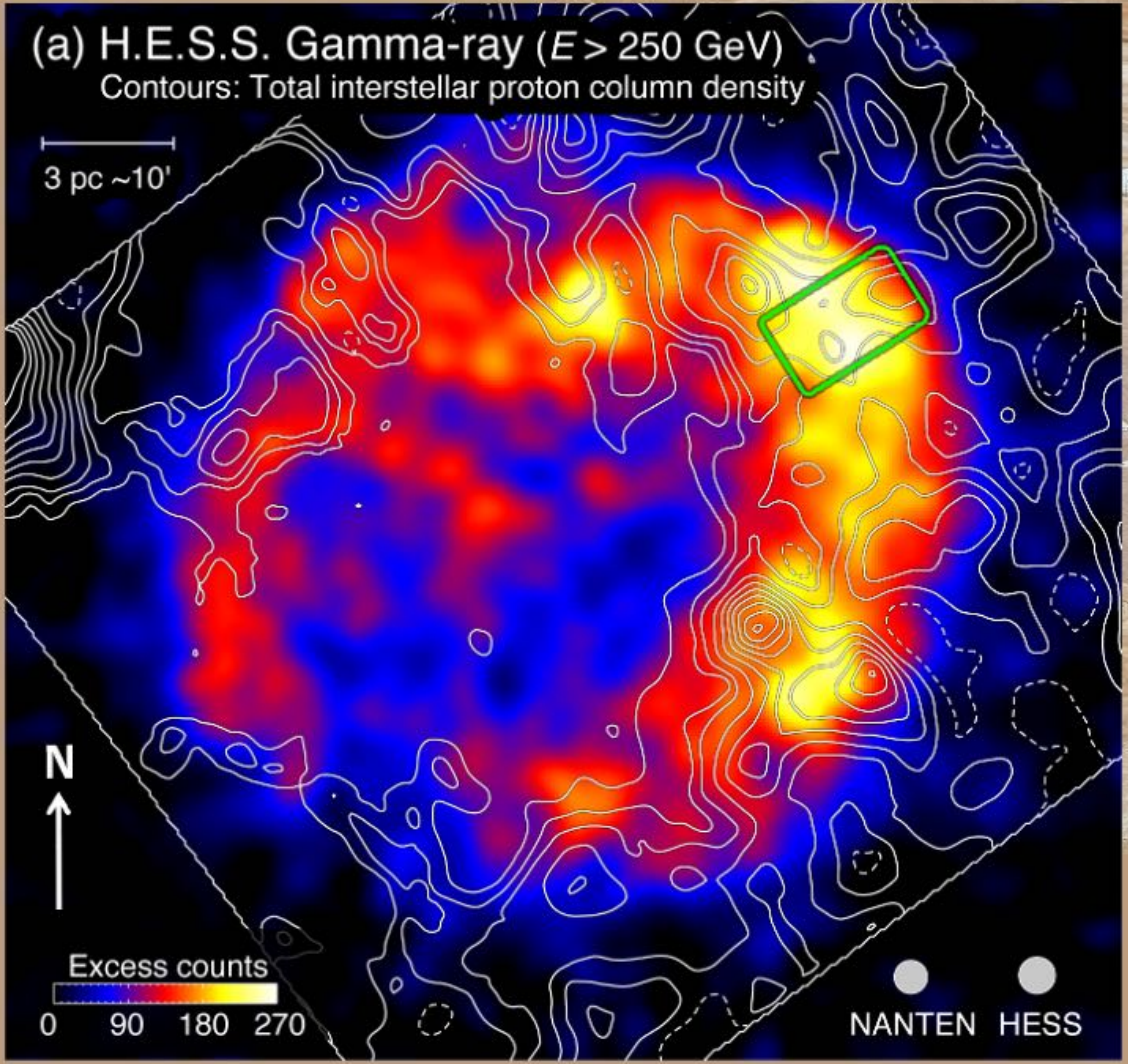

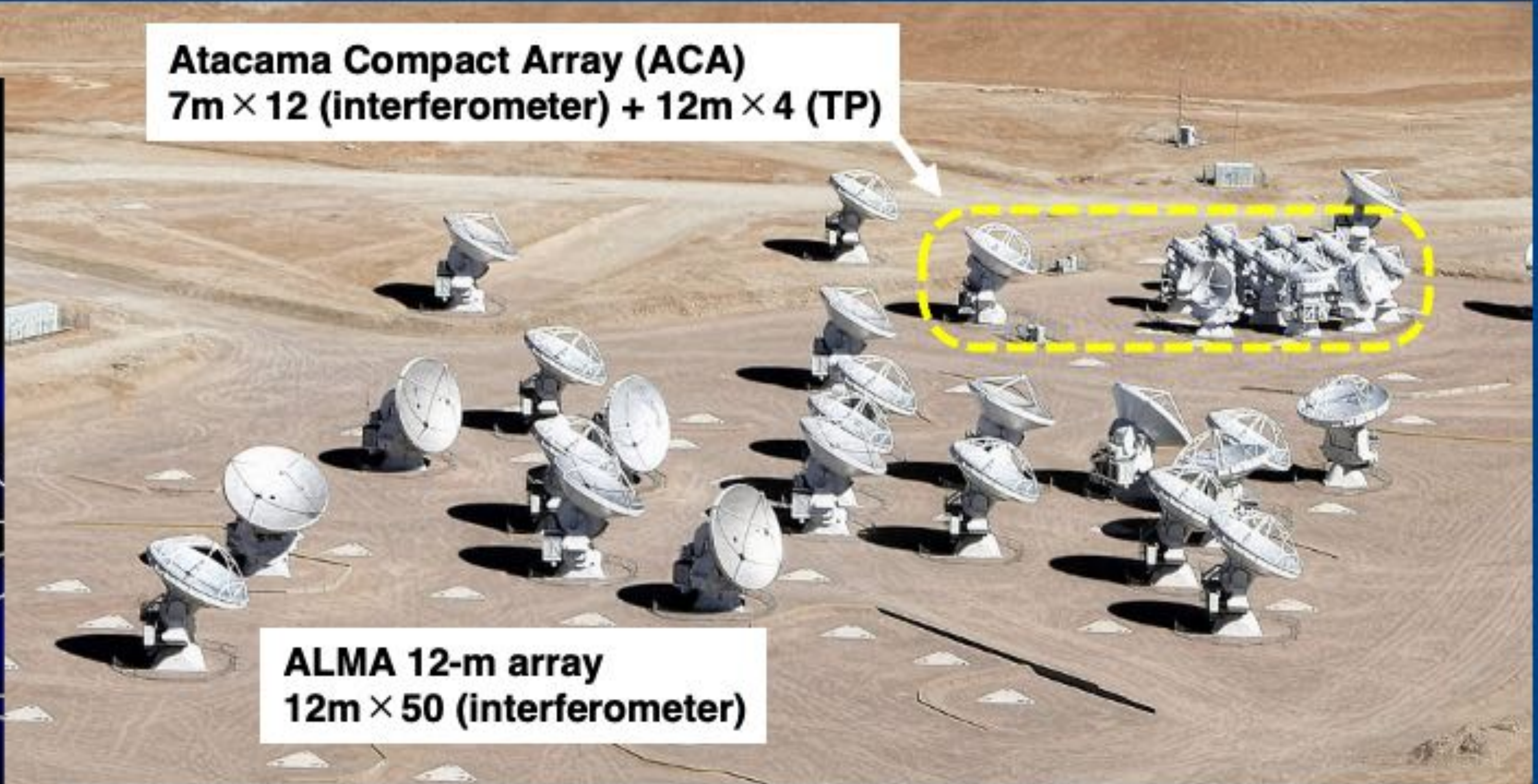

Atacama Compact Array (ACA)
7m × 12 (interferometer) + 12m × 4 (TP)

ALMA 12-m array
12m × 50 (interferometer)

Project# (Cycle / PI)	2017.1.01406.S (Cycle 5 / H.Sano)
Target line	^{12}CO (J = 1–0)
Observed area	11.1' × 6.4' (mosaic mode)
Antennas	12-m array + ACA (7-m array + TP)
Observing time	**5.3 hrs (12-m) + 45.3 hrs (ACA)**
Baseline (u-v dist.)	8.9–313.7 m (3.4–120.6 $k\lambda$)
Beam size	**4.37" × 3.89" (~0.02 pc)**
RMS noise level	~ 0.13 K @ 0.4 km s^{-1}

Results 1: Overview of ALMA CO observations

Sano et al. 2020c, ApJL, 904, L24

Results 2: Cloudlets survived from the wind/shock erosion

Size: ~0.06–0.10 pc
Mass: ~0.1-0.5 $M_{\odot}$
Density: ~10^4 cm^{-3}

Image: ALMA CO
Contours: Chandra X-ray
Crosses: X-ray hotspots

Results 3: Distributions of X-ray hot spots and cloudlets

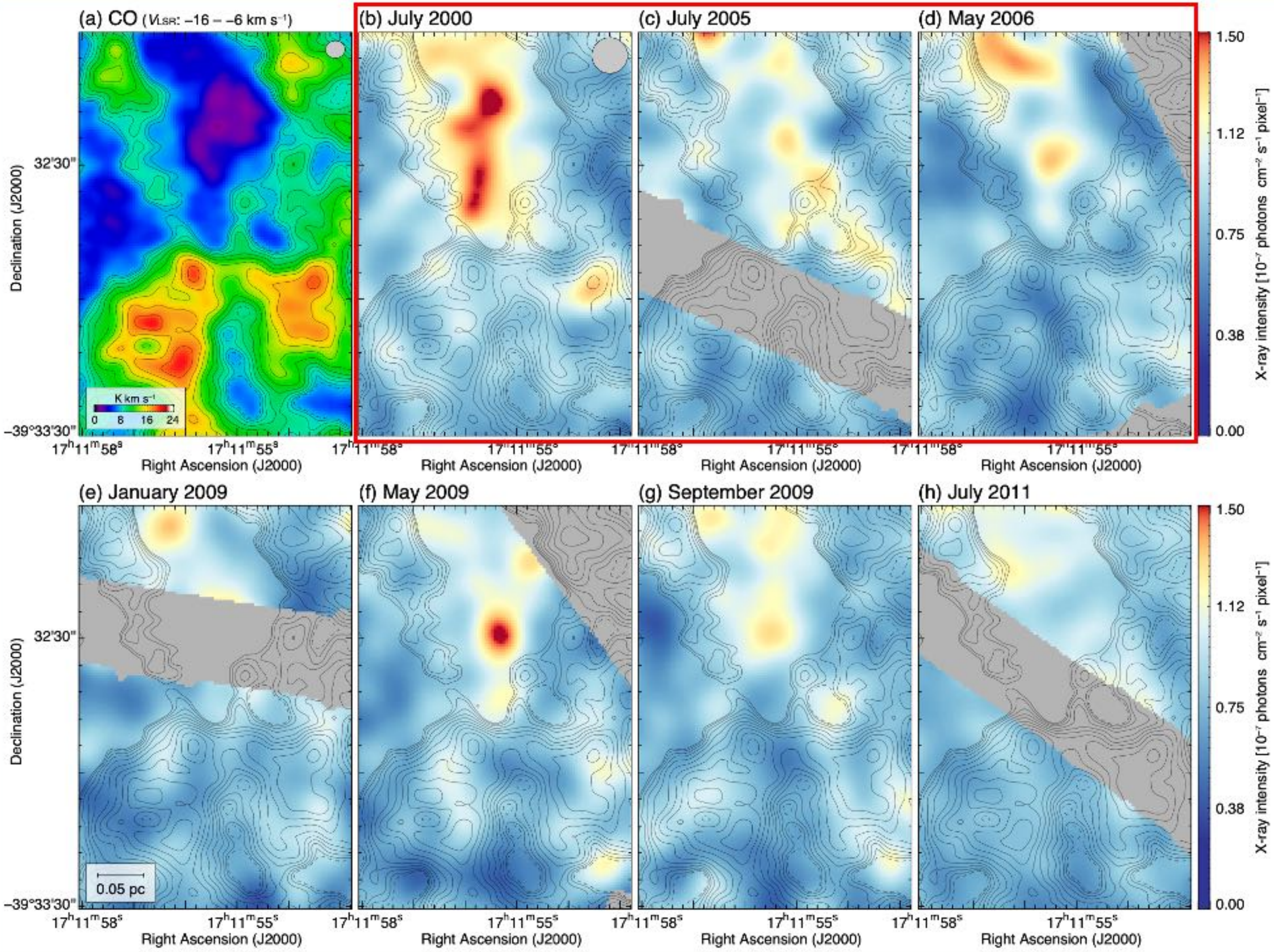

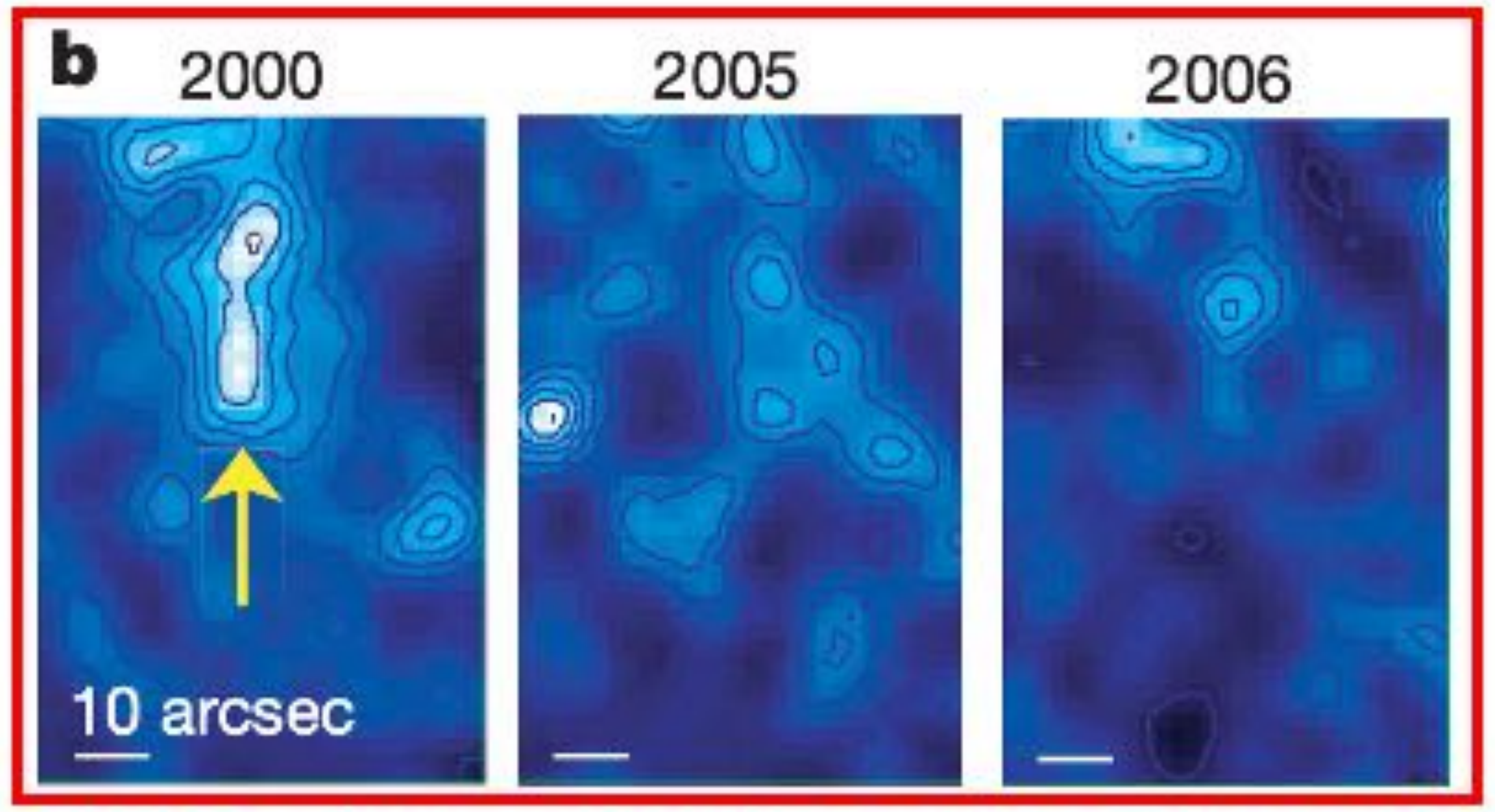

Almost the same area that presented in Uchiyama et al. (2007)

New hotspot on May 09 (~4σ)

➡ B ~0.3–3 mG

acceleration time < three years

cooling time < four months

Separation between clouds and hotspots: ~0.05–0.15 pc

Image: (a) ALMA CO ($V_{\rm LSR}$: −16–6 km s^{-1})
(b–h) *Chandra* X-rays (E: 2–7 keV)
Contours: ALMA CO ($V_{\rm LSR}$: −16–6 km s^{-1})

Sano et al. 2020c, ApJL, 904, L24

Discussion 1: *B* amplification via shock-cloudlet interactions

Spatial correspondence between X-ray hotspots and cloudlets cloud be understood as a result of the shock-cloud interaction
→ Celli et al. (2019) provides with us a numerical support!

	Celli+2019	This study
Cloud size [pc]	0.2	~0.06–0.10
Cloud density [cm^{-3}]	10^3	~10^4
Inter-cloud density [cm^{-3}]	0.01	~0.1
ISM density contrast	10^5	~10^5
B field or X-ray amplification	mainly cloud surroundings	cloudlets surroundings
Separation: cloud–$B_{\max}$ [pc]	~0.4	-------
Separation: cloud–hotspots [pc]	-------	~0.05–0.15

When we scaled the Celli's cloud to observed values ~0.06–0.10 pc, separation between the cloud and $B_{\max}$ to be ~0.12–0.20 pc, which is consistent with the observed values of ~0.05–0.15 pc.

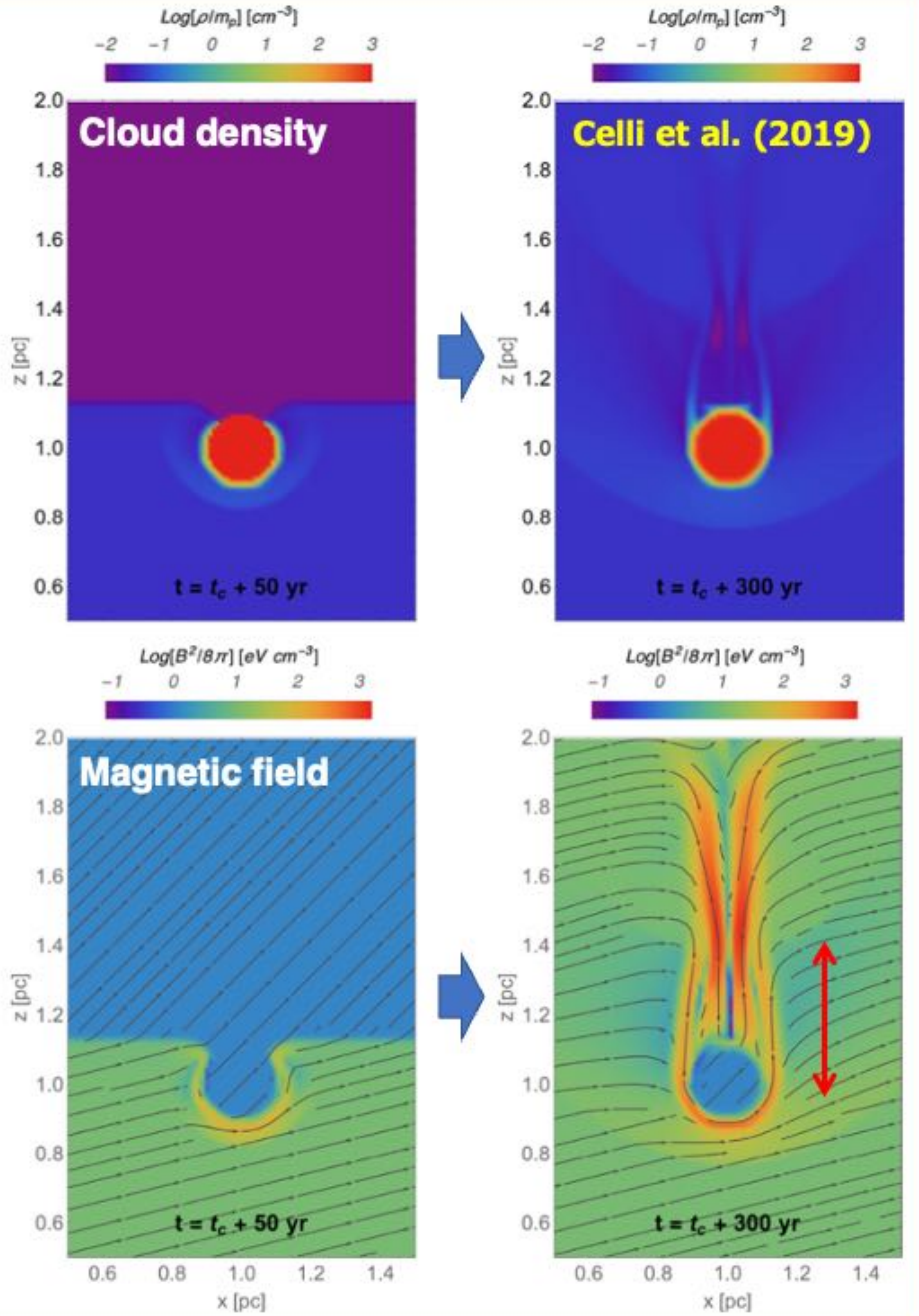

Discussion 2: Modulation of gamma-ray spectrum

$$l_{\rm pd} \simeq (\kappa_{\rm d}\, t)^{1/2} = 0.1\,\eta^{1/2}\left(\frac{E}{10\ {\rm TeV}}\right)^{1/2}\left(\frac{B}{100\ \mu{\rm G}}\right)^{-1/2}\left(\frac{t_{\rm age}}{10^3\ {\rm yr}}\right)^{1/2}\ {\rm pc},$$

Inoue et al. (2012)

$l_{\rm pd}$: penetration depth,
η: gyro factor,
E: CR proton energy,
B: magnetic field,
$t_{\rm age}$: SNR age

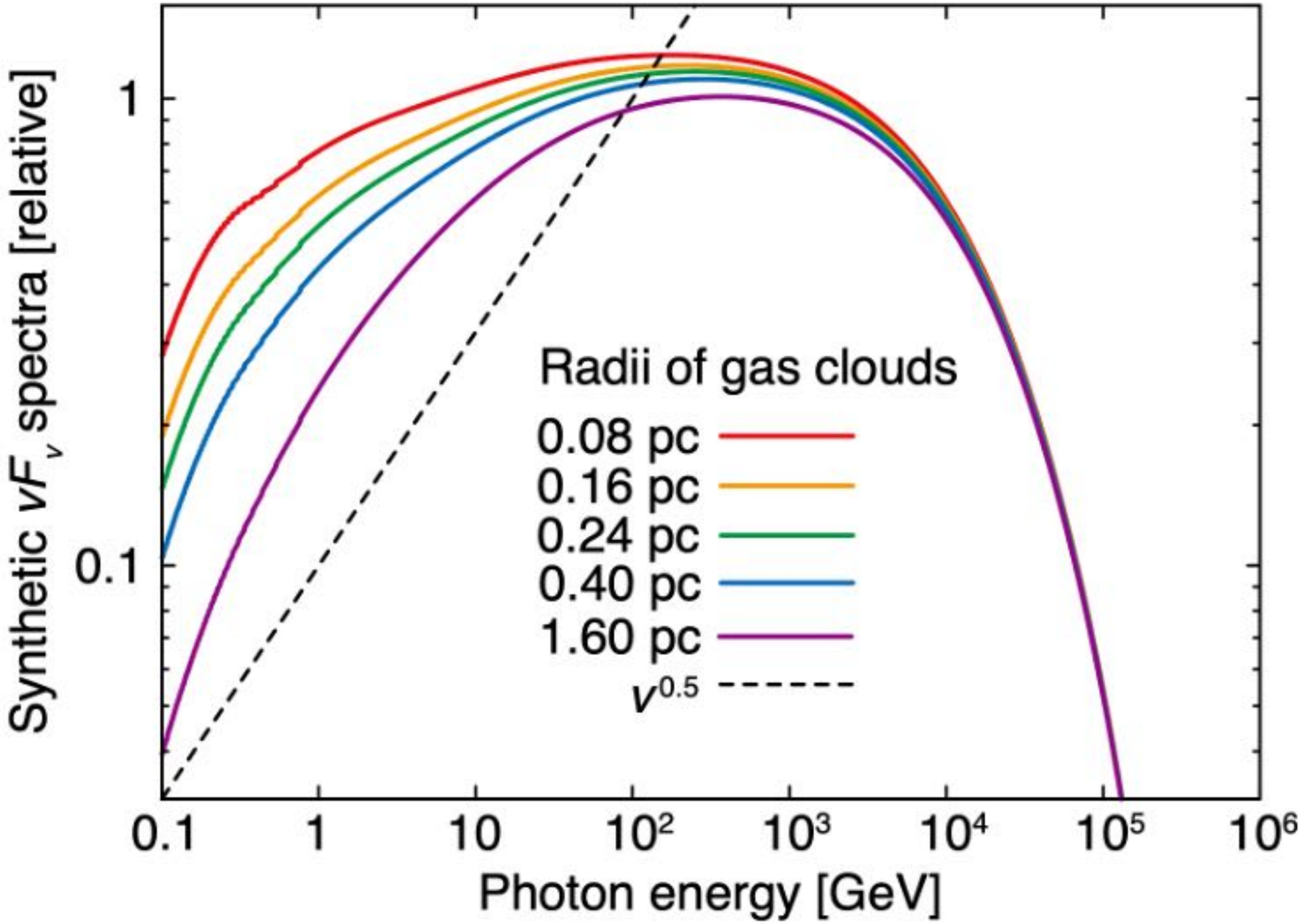

Flatter νF_ν gamma-ray spectra will be expected toward the NW of RXJ1713

*Typical cloud radii are ~1–2 pc (Moriguchi+05)
e.g., CO cloud "peak C" (~1.5 pc) shows density concentration without small-scall structure

*Typical radii of cloudlets in the RXJ1713 NW are ~0.03–0.05 pc (this study)

Further gamma-ray observations with high-spatial resolution and sensitivity will reveal the gamma-ray spectral modulation...!!

Sano et al. 2020c, ApJL, 904, L24

Quantifying the Hadronic & Leptonic Gamma-rays ➡ e-poster #490

Pursuing the Origin of the Gamma Rays in RX J1713.7-3946 Quantifying the Hadronic and Leptonic Components

Yasuo Fukui[1], **Hidetoshi Sano**[2], Yumiko Yamane[1], Takahiro Hayakawa[1], Tsuyohi Inoue[3], Kengo Tachihara[1], Gavin Rowell[4], Sabrina Einecke[4]

[1]*Department of Physics, Nagoya University, Furo-cho, Chikusa-ku, Nagoya 464-8601, Japan (fukui@a.phys.nagoya-u.ac.jp)*
[2]*Faculty of Engineering, Gifu University, 1-1 Yanagido, Gifu 501-1193, Japan (hsano@gifu-u.ac.jp)*
[3]*Department of Physics, Konan University, Okamoto 8-9-1, Kobe, Japan*
[4]*School of Physical Sciences, The University of Adelaide, North Terrace, Adelaide, SA 5005, Australia*

This study has been published in The Astrophysical Journal
Fukui et al. (2021), ApJ, 915, 84 Journal link QR code ➡

1. Cosmic-rays & Supernova Remnants

☑ It is a longstanding question how cosmic-ray (CR) protons are accelerated in interstellar space.

☑ Supernova remnants (SNRs) are the most likely candidates for acceleration because the high-speed shock waves offer an ideal site for the DSA [e.g.,1,2].

2. Hadronic gamma-rays from young SNRs

☑ TeV gamma-rays from young SNRs are mainly produced by relativistic CR protons and/or electrons close to PeV through two mechanisms, called hadronic or leptonic processes (Fig.1).

☑ Numerous attempts have been made to distinguish the two processes using broadband spectral modeling [e.g.,3]. In most cases, however, it is difficult to distinguish between hadronic and leptonic gamma-rays by the spectral modeling alone (Fig.1., [e.g., 3,4,5]).

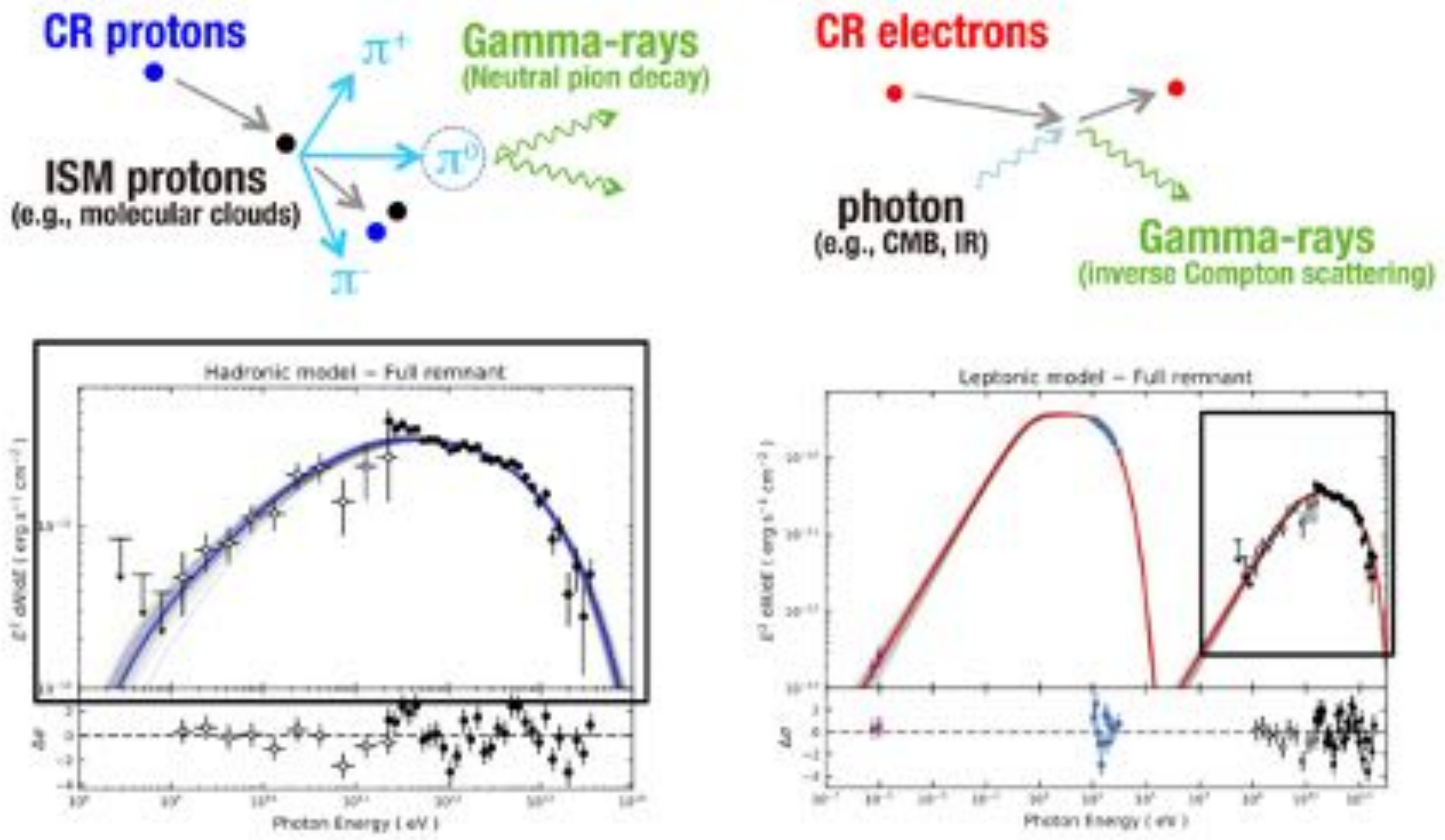

Fig. 1: (upper panels) Schematic images of hadronic and leptonic gamma-rays. (lower panels) Results of spectral modeling toward the TeV gamma-ray SNR RX J1713.7−3946 by H.E.S.S. collaboration et al. [3].

3. Spatial correspondence between the ISM protons & gamma-rays

☑ The hadronic gamma-ray flux is proportional to the target-gas density.

☑ We presented good spatial correspondence between TeV gamma-rays and ISM protons in the young SNRs RX J1713.7–3946, Vela Jr., HESS J1731-347, and RCW 86. This provides one of the essential conditions for gamma-rays to be predominantly of hadronic origin [6-9].

☑ The total energy of CR protons, ~10^{48}–10^{49} erg, derived using ISM density gives a lower limit.

Open question: How much do leptonic gamma-rays contribute to the total gamma-rays?

The gamma-rays from these SNRs are mainly of hadronic origin, while a contribution from the leptonic component was not excluded. We aim to quantify the hadronic and leptonic gamma-rays by imaging analysis of the gamma-ray, X-ray, and the ISM in RXJ1713.

4. A novel imaging analysis of radio, X-ray, and gamma-ray radiation in RXJ1713

☑ We propose a new methodology that assumes that the number of gamma-ray counts N_g is expressed as a linear combination of two terms: one (hadronic gamma-ray) is proportional to the ISM column density N_p and the other (leptonic gamma-ray) is proportional to the X-ray count N_x (see Fig.2, [10]).

☑ By fitting the expression to the data pixels, we find that the gamma-ray counts are well represented by a tilted flat plane in a 3D space of N_p–N_x–N_g. This plane illustrates that the total number of gamma rays N_g increases with N_p and N_x, respectively, which is consistent with the hybrid picture.

☑ The results show that the hadronic and leptonic components occupy (58–70)% and (25–37)% of the total gamma rays, respectively ➡ **Further support for the acceleration of the CR protons!**

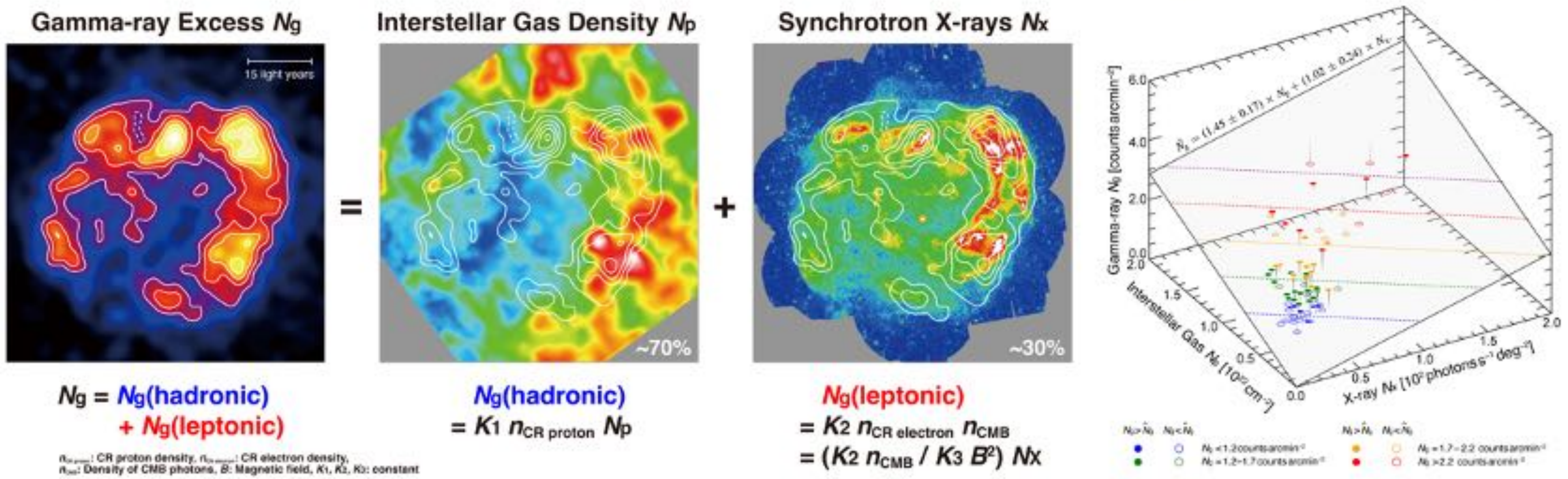

$N_g = N_g$(hadronic) + N_g(leptonic)

N_g(hadronic) $= K_1\, n_{\mathrm{CR\ proton}}\, N_p$

N_g(leptonic) $= K_2\, n_{\mathrm{CR\ electron}}\, n_{\mathrm{CMB}} = (K_2\, n_{\mathrm{CMB}} / K_3 B^2)\, N_X$

$n_{\mathrm{CR\ proton}}$: CR proton density, $n_{\mathrm{CR\ electron}}$: CR electron density, n_{CMB}: Density of CMB photons, B: Magnetic field, K_1, K_2, K_3: constant

Fig. 2: (Left three images) Maps of the H.E.S.S. TeV gamma-rays N_g (left, E > 2 TeV, [3]), total interstellar proton column density N_p (middle, [6]), and the XMM-Newton synchrotron X-rays (right, E: 1.0–5.0 keV) in the SNR RX J1713.7−3946. (Right panel) 3D fitting of a flat plane in the N_p–N_x–N_g space with a pixel size of 4.8 arcmin. The data pixels are colored by the code in the figure according to N_g, and are shown by filled and open symbols for those above and below the plane. Each vertical line connects N_g and $\hat{N}_g$ where the hat symbol on N_g means that it is predicted by the regression. The blue, green, orange, red, and purple lines on the best-fit plane indicate $\hat{N}_g$ = 1.0, 1.5, 2.0, 2.5, and 3.0 cnt arcmin^{-2}, respectively.

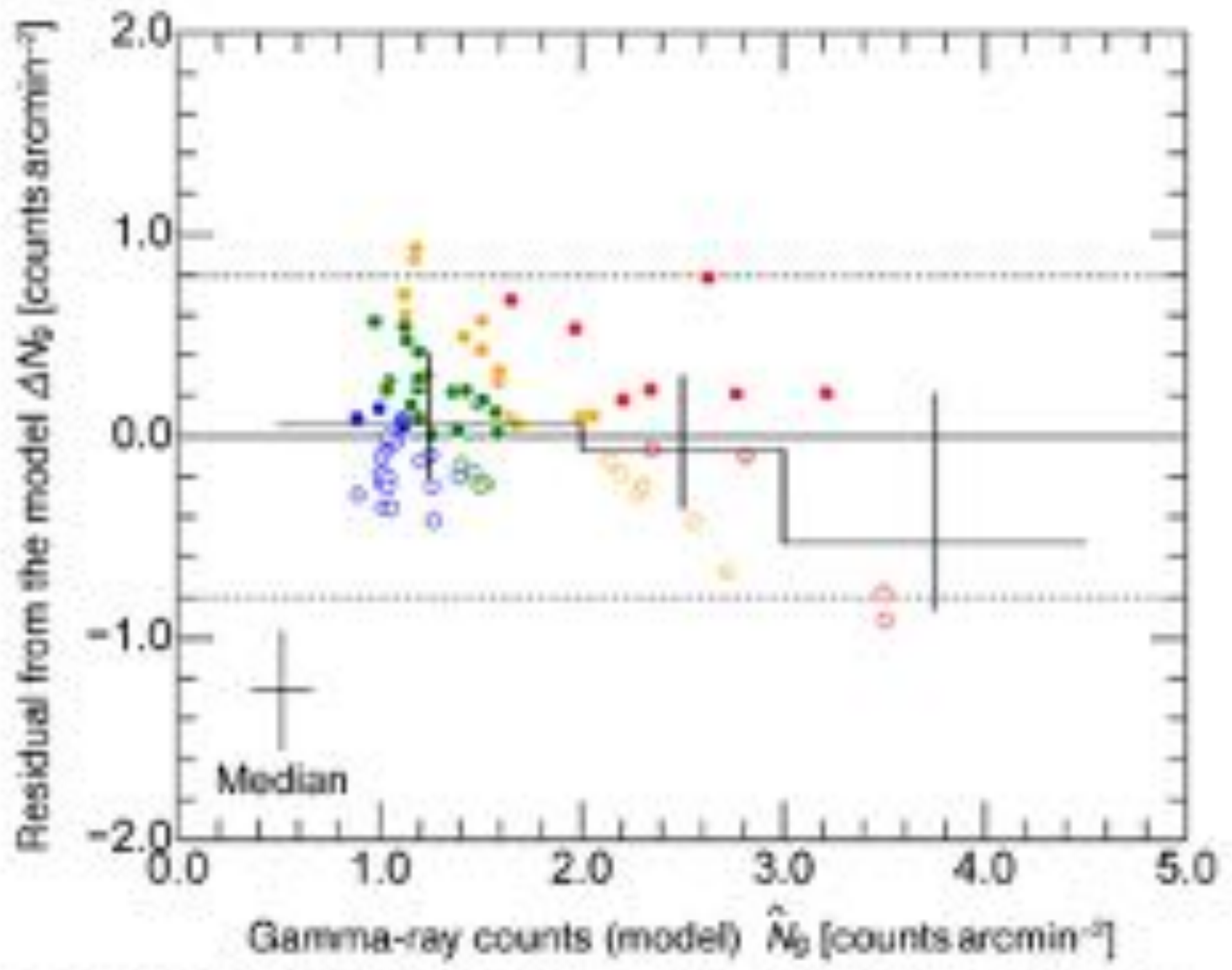

Fig. 3: Plot of the difference $\Delta N_g = N_g - \hat{N}_g$ with respect to $\hat{N}_g$. The averages of ΔN_g weighted with $\sigma(\Delta N_g)^{-2}$ are shown for three bins of $\hat{N}_g$ with the vertical error bars.

5. Discussion and Future Prospects

☑ There is a marginal hint that the gamma rays are suppressed at high gamma-ray counts (see Fig. 3), which may be ascribed to second-order effects including the **shock–cloud interaction** and the effect of penetration depth. **The shock–cloud interaction excites turbulence toward the dense cores and amplifies the magnetic field up to 100 μG ➡ Suppression of the leptonic gamma-rays**

☑ CR protons cannot penetrate into the dense cores because of their limited penetration depth around dense cores where the turbulent magnetic field reduces the CR diffusion. This reduces the hadronic gamma-rays toward the dense cores. Since Sano et al. (2020) [11] also showed clumpy clouds with a size of 0.01 pc scales, a high-resolution ISM study is needed to understand the gamma-ray spectra.
➡ Follow-up observations using ALMA and CTA will solve the issues

☑ The methodology proposed in the present work has provided a new tool to quantify the leptonic and hadronic gamma-rays and will be applicable to the other gamma-ray bright SNRs. In any case, investigating the ISM associated with gamma-ray SNRs are crucial in understanding the origin of gamma-rays.

6. References

[1] Bell 1978, MNRAS, 182, 147, [2] Blandford & Ostriker (1978), ApJL, 221, 29, [3] H.E.S.S. Collaboration (2018), A&A, 612, A6, [4] H.E.S.S. Collaboration (2018), A&A, 612, A12, [5] Inoue et al. (2012), ApJ, 744, [6] Fukui et al. (2012), ApJ, 746, 82, [7] Fukui et al. (2017), ApJ, 850, 71, [8] Sano et al. (2019), ApJ, 876, 37, [9] Fukuda et al. (2014), ApJ, 788, 94, [10] Fukui et al. (2021), ApJ, 915, 84, [11] Sano et al. (2020), ApJL, 904, L24 ➡ see also the contributed talk #462 (7th July 2022, 16:00–16:15).

Summary

- **Shock-cloud interaction**

  Investigating the interstellar molecular/atomic clouds associated with supernova remnants play an essential role in understanding particle acceleration and its radiation.

- **ALMA CO observations in the NW-rm of RXJ1713 (Sano et al. 2020c, ApJL, 904, 24)**
  - Numerous molecular cloudlets (size: ~0.01 pc, density: $\sim 10^4$ cm^{-3}) within a wind bubble, which are physically associated with both the X-ray filaments and hotspots.
  - The spatial separation between X-ray hotspots and cloudlets are roughly consistent with the numerical results of shock-cloud interactions (e.g., Celli et al. 2019), suggesting that shock-cloudlet interaction with B field amplification occurred.
  - Gamma-ray spectral modulation is also expected (see Inoue 2019).

- **Quantifying the Hadronic & Leptonic Gamma-rays (e-poster #490)**
  - We propose a new methodology that assumes that the number of gamma-ray counts is expressed as a linear combination of two terms: one is proportional to the ISM density and the other proportional to the synchrotron X-ray counts
  - The hadronic & leptonic comps. occupy 70% & 30% of the total gamma-rays, respectively.